Influence of electron releasing groups in benzylidene thiocarbohydrazide and their synergistic effect with iodide ions on acidizing corrosion inhibition of carbon steel in 15% HCl solution - Experimental and theoretical approach

Sathiya Priya Jayakumar[1], Vignesh Murugadoss[2] & Subramania Angaiah*[1,2]

[1]Advanced Materials Research Lab, Department of Industrial Chemistry, Alagappa University, Karaikudi 630 003, India.
[2]Electro-Materials Research Laboratory, Centre for Nanoscience and Technology, Pondicherry University, Puducherry 605 014, India.

E-mail: a.subramania@gmail.com

Influence of electron releasing groups in benzylidene thiocarbohydrazide and their synergetic effect with iodide ions on acidizing corrosion inhibition of carbon steel in 15% HCl using chemical and electrochemical methods has been studied. Tafel polarization measurements indicate that these compounds act as mixed-type inhibitors. The adsorption of these compounds obey Langmuir adsorption isotherm and the thermodynamic parameters are also calculated to explain their inhibitive action. The increase in synergism parameter (S_θ) indicates that the inhibition efficiency is improved in the presence of the iodide ions. Further, the density functional theory is used to validate the experimental results.

Keywords: Acidizing inhibitors, Adsorption isotherm, Carbon steel, HCl, Synergic effect, Quantum chemical studies

Acidization of petroleum oil well is one of the important simulation techniques for enhancing oil production[1-4]. It is commonly brought by forcing a solution of about 15-20% HCl acid into the well through N80 steel turbine to remove plugging in the bore well and stimulate production in the petroleum industry[5-7]. These steel tubing gets corroded during acidization. To avoid this aggressive attack of the acid on tubing and casting materials, inhibitors are added to the acid solution during this acidization process[8,9]. The choice of inhibitors depends upon the acids and also its inhibition at higher temperatures. Organic compounds containing N, O or S groups or organic compounds having bonds in their structures are found to be effective inhibitors in acid media[10-14]. Presence of functional groups, such as =NH, -N=N-, -CHO, R-OH, C = C, etc., in the inhibitor molecule and also the steric factors, aromaticity, electron density at the donor atoms are found to influence the adsorption of the inhibitor molecule over corroding metal surface[15-18].

Effective acidizing inhibitors that are usually found in commercial formulations are acetylenic alcohols, alkenyl phenones, aromatic aldehydes, nitrogen-containing heterocycles, and their quaternary salts, condensation products of carbonyl compounds and amines, etc[19-27]. The choice of effective inhibitors has been mostly done by using empirical knowledge based on their mechanism of action and electron-donating ability. Amines and their derivatives are well-known corrosion inhibitors and can effectively protect metals from corrosion.

The synergistic influence of iodide ions with different organic inhibitors in acid solutions has been studied by several authors[28,29]. Corrosion inhibition in hydrochloric acid solution has been studied using combinations of metal halides and organic inhibitors. Inhibition is sensitive to the type of metal halides used. Various metal halides are studied with an amine base organic corrosion inhibitor. Cuprous iodide inhibited corrosion better than the other metal halides. The efficiency of amine-type inhibitors in acidizing solutions based on hydrochloric acid can be markedly improved by adding metal halides, especially copper (I) iodide. In the present investigation, acidizing inhibitors are synthesized with a view to finding a new cost-effective acidizing inhibitor that can effectively control the corrosion of oil-well equipment during acidization. The corrosion inhibiting action of synthesized compounds has been evaluated by weight loss, electrochemical and hydrogen permeation studies. The synergistic effect is carried out at the optimum concentration of inhibitors with various concentrations of KI and CuI. Further, it is intended to

study the influence of substituted electron releasing groups in benzylidene thiocarbohydrazide derivatives on the corrosion inhibition efficiency. Further, the density functional theory is used to validate the experimental results.

Experimental Section

Material preparation

Carbon steel strips of size $4.5 \times 2 \times 0.2$cm containing 0.14% C, 0.35% Mn, 0.17% Si, 0.025% S, 0.03% P and the remainder Fe were used for weight loss and hydrogen permeation studies. For electrochemical studies, carbon steel strips of the same composition with an exposed area of 1 cm^2 were used. Carbon steel strips were polished mechanically with emery papers of 1/0 to 4/0 grades. They were subsequently degreased with trichloroethylene before use. Analytical reagent (AR) - grade HCl (Merck) and double distilled water were used for preparing 15% HCl. All other chemicals used for synthesizing inhibitors were from analytical reagent grade only.

Synthesis of acidizing inhibitors

Preparation of 1-benzylidene-3-thiocarbohydrazide (BTCH)

10.6 g (0.1moL) of thiocarbohydrazide was dissolved in 200 mL hot water and treated with 10.1 mL of benzaldehyde (0.1mol) in ethanol (30 mL) dropwise with constant stirring for 20 min at 50°C, then the mixture was allowed to stand overnight to give a yellow coloured solid compound namely, 1-benzylidene-3-thiocarbohydrazide (BTCH). Thus obtained 1-benzylidene -3-thiocarbohydrazide was recrystallized with an equal ratio of acetone and ethanol to get pure yellow crystalline solid.

Similarly, other aromatic aldehydes such as salicylaldehyde and anisaldehyde were condensed with thiocarbohydrazide in respective proportions to get 1-salicylidene-3-thiocarbohydrazide (STCH) and 1- anisylidene-3-thiocarbohydrazide (ATCH) respectively. These synthesized compounds are solids and their melting points were determined using the melting point apparatus. The molecular formula, molecular weight, molecular structure and melting point of the synthesized acidizing inhibitors are given in Table 1.

Characterization of acidizing Inhibitors

UV-Visible spectral studies

The UV-Visible absorption spectra were recorded by dissolving a small quantity of the prepared acidizing inhibitors in acetone using Shimadzu (UV-2401) UV-Visible spectrophotometer. Before

spectroscopic measurements, the baseline correction was made suitably using acetone. The spectra were recorded in the range between 300-800nm. The spectrum for the precursors was also run to ensure the formation of the compounds.

FTIR spectral studies

FTIR spectra were recorded for the synthesized acidizing inhibitors to confirm the condensation products obtained by condensing thiocarbohydrazide with benzaldehyde/salicylaldehyde/anisaldehyde using Perkin-Elmer FTIR Spectrophotometer (Paragon Model 500).

Non-electrochemical methods

Weight loss measurements

Carbon steel specimens were immersed in 100ml of inhibited and uninhibited solutions for 6h at 30°C. The corrosion rate (mmpy) and inhibition efficiencies were calculated from the difference in weight loss values in the absence and presence of inhibitors in 15% HCl solution using the following equations[30];

$$\text{Corrosion rate (mmpy)} = \frac{KW}{ATD} \qquad \ldots (1)$$

where K is the constant of 8.76×10^4, W is the weight loss in g, A is the area in cm^2, T is the time in h and D is the density in gm /cm^3 (7.86).

$$\text{Inhibition efficiency (\%)} = \frac{W_B - W_I}{W_B} \times 100 \qquad \ldots (2)$$

where W_B and W_I are weight loss per unit time in the absence and presence of inhibitors.

The degree of surface coverage (θ) was also calculated from the weight loss measurement results using the formula[31];

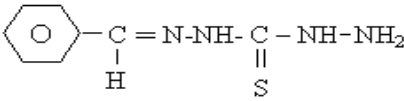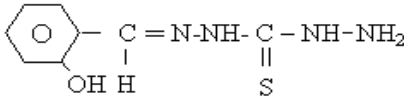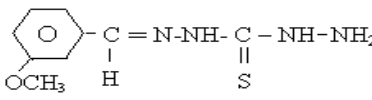$$\text{Surface coverage (\%)} = \frac{W_B - W_I}{W_B} \times 100 \qquad \ldots (3)$$

where W_B is the weight loss in the absence of inhibitor and W_I is the weight loss in the presence of inhibitor.

Electrochemical methods

Electrochemical polarization studies

Polarization studies were carried out using an EG & G-Electrochemical analyzer (Model-6310) in a conventional three-electrode glass cell. Carbon steel strips of the same composition with an exposed area of 1cm^2 were used as the working electrode. A platinum foil of surface area 2cm^2 was used as the

Table 1 — Molecular formula, molecular weight, structure and melting point of the synthesized organic compounds

Name of the acidizing inhibitor	Molecular Formula	Molecular weight	Structure	Melting point (°C)
1-Benzylidene-3-thiocarbohydrazide (BTCH)	$C_8H_{10}N_4S$	194.18		121
1-Salicylidene-3-thiocarbohydrazide (STCH)	$C_8H_{10}N_4SO$	210.18		210
1- Anisylidene-3-thiocarbohydrazide (ATCH)	$C_9H_{12}N_4SO$	224.19		150

auxiliary and saturated calomel electrode (SCE) as the reference. The working electrode was first immersed in the test solution for 10-15min to establish a steady open-circuit potential, then the runs were carried out with a potential range ± 250 mV with respect to open circuit potential (OCP) at a scan rate of 1 mVs^{-1}. Both anodic and cathodic polarization curves were recorded in the absence and presence of different concentrations of inhibitors. The inhibition efficiencies of synthesized inhibitors by polarization method were calculated using the following equation[32];

$$IE\ (\%)= \frac{I_{Corr}- I_{Corr}^*}{I_{Corr}} \times 100 \qquad \dots (4)$$

where I_{corr} and I^*_{corr} are corrosion current in the absence and presence of inhibitors, determined by extrapolation of cathodic and anodic Tafel lines to the corrosion potential.

Electrochemical ac-impedance studies

The electrochemical ac-impedance measurements were performed using the EG&G Electrochemical impedance analyzer (Model-6310). A time interval of 10-15 min was given to attain the steady-state open circuit potential, then the a.c impedance measurements carried at the open circuit potential. A sine wave voltage (10mV) was superimposed on the resting potential. The real part (Z') and the imaginary part (Z") were measured at various frequencies in the range of 100 kHz to 10 mHz. From the plots, the charge transfer resistance (R_t) were calculated and then the double layer capacitance was calculated using the following equation[33];

$$C_{dl}= {}^1\!/_{2\pi f_{max}R_t} \qquad \dots (5)$$

where R_t is the charge transfer resistance and C_{dl} is the double layer capacitance

The experiments were carried out in the absence and presence of different concentrations of inhibitors. The percentage of inhibition efficiency was calculated using the following equation[34];

$$IE(\%)= \frac{R_t^*-R_t}{R_t^*} \qquad \dots (6)$$

where R_t^* and R_t are the charge transfer resistance in the presence and absence of inhibitors.

Effect of temperatures

To study the effect of temperature on corrosion of carbon steel in 15% HCl solution, weight loss measurements were made at temperatures ranging from 30°C to 110°C for an immersion period of 1 hour in the absence and presence of different concentrations of inhibitors.

Synergistic effect of acidizing inhibitors with KI /CuI

The synergistic effect caused by potassium iodide and copper iodide on the inhibition of carbon steel in 15% boiling HCl in the presence of a best inhibiting concentration of inhibitors was also studied at 110ºC using weight loss measurements.

Hydrogen permeation studies

The hydrogen permeation study was carried out using an adaptation of the modified two-compartment cell described earlier[35,36]. The specimen used for the study was a thin carbon steel membrane which was fixed in between two compartments using Teflon bush and then clamped tightly. A Hg/HgO/0.2N NaOH was used as the reference electrode and Pt as a counter electrode. The anodic side of the carbon steel

membrane was electroplated with a thin layer of Pd. On the cathodic compartment, the test solution was taken and was then allowed to corrode at a constant potential of –300 mV, which is the most suitable potential for ionizing the diffused hydrogen rapidly and efficiently. A part of hydrogen produced could penetrate through the membrane and get ionized at the Pd/0.2N NaOH interface which is accounted as permeation current using X–Y/t recorder. The permeation current was measured in 15% HCl medium in the absence and presence of inhibitors of the best inhibiting concentration of the inhibitors.

Surface examination study

The carbon steel specimens were immersed in a 15% HCl solution in the absence and presence of the best inhibiting concentration of the inhibitors for 6h. After 6h, the specimens were taken out and dried. The nature of the film formed on the metal surface was analyzed by the following surface analytical techniques.

Analysis of FT-IR spectra

The FT-IR spectra were recorded using Perkin-Elmer (Paragon Model - 500) FT-IR spectrophotometer for the carbon steel surface immersed in 15% HCl solution in the absence and presence of the best inhibiting concentration of inhibitors.

Analysis of UV-Visible reflectance

UV-Visible reflectance spectral studies were made on the surface of polished, corroded and corrosion-inhibited carbon steel specimens in the region of 200 to 800nm using Hitachi (Model U - 3400) UV-Visible - NIR spectrophotometer.

Scanning electron microscopic studies

Surface examination of carbon steel specimens was made using JEOL–Scanning electron microscope (SEM) with the magnification of 1000x for the carbon steel specimens immersed in 15% HCl solution for six hours at 30°C in the absence and presence of the best inhibiting concentration of inhibitors.

Quantum chemical calculation studies

Quantum chemical calculations were performed in Gaussian 09 software for Windows. The molecules of the prepared acidizing inhibitors were geometrically optimized using the density functional theory (DFT) approach involving B3LYP (Becke three-parameter functional along with the Lee-Yang-Paar correlation) with 6-31G (d, p) basis set. The energies for the frontier molecular orbitals, E_{HOMO} (HOMO - highest occupied molecular orbital energy) and E_{LUMO} (LUMO - lowest unoccupied molecular orbital energy) were obtained. Other theoretical parameters such as the energy gap (ΔE), global electronegativity (χ), global Hardness (η), global Softness (σ) and the fraction of electrons transferred from the inhibitor to the metal (ΔN) were calculated from the following equations[37-39];

Energy gap (ΔE) = $E_{LUMO} - E_{HOMO}$ … (7)

Global electronegativity (χ) = -0.5 x ($E_{LUMO} + E_{HOMO}$)
                                                          … (8)

Global Hardness (η) = 0.5 x ($E_{LUMO} - E_{HOMO}$)   … (9)

Global Softness (σ) = 1/ η … (10)

Fraction of electrons transferred from the

inhibitor to the metal atom (ΔN) = $\dfrac{\chi_{Fe} - \chi_{inhibitor}}{2\,(\eta_{Fe} - \eta_{inhibitor})}$
                                                          … (11)

where χ_{Fe} and η_{Fe} are the global electronegativity and global Hardness of the iron, respectively. The reported values of 7 eV/mol and 0 eV/mol were used in calculations for χ_{Fe} and η_{Fe}, respectively.

Results

Characterization of synthesized acidizing Inhibitors
UV- Visible spectral studies

The UV-Visible spectra of BTCH, STCH, and ATCH in acetone showed absorption bands at 376, 387 and 375 nm, characteristic of n-π^{*} transition confirming the presence of C = N group in the molecule. Absorption bands in the region of 250-360 nm are characteristic of C = N group. In the case of synthesized compounds, the absorption maximum is slightly shifted towards longer wavelength (Bathochromic shift) due to the presence of auxochrome (NH$_2$) group.

FTIR spectral studies

The absorption frequencies in the range of 1690-1640 cm^{-1} are characteristic of azomethine group >C = N-. In the case of synthesized compounds, the >C = N- stretching vibration frequency is shifted slightly towards lower frequency due to the delocalization of π electrons in the benzene ring and lone pair of electrons present on N and S atoms. Thus, the basic >C = N- stretching vibrations are present at 1600, 1619 and 1622 cm^{-1} for BTCH, ATCH, and STCH, respectivelyand their corresponding spectrums are given in Fig. 1(a-c).
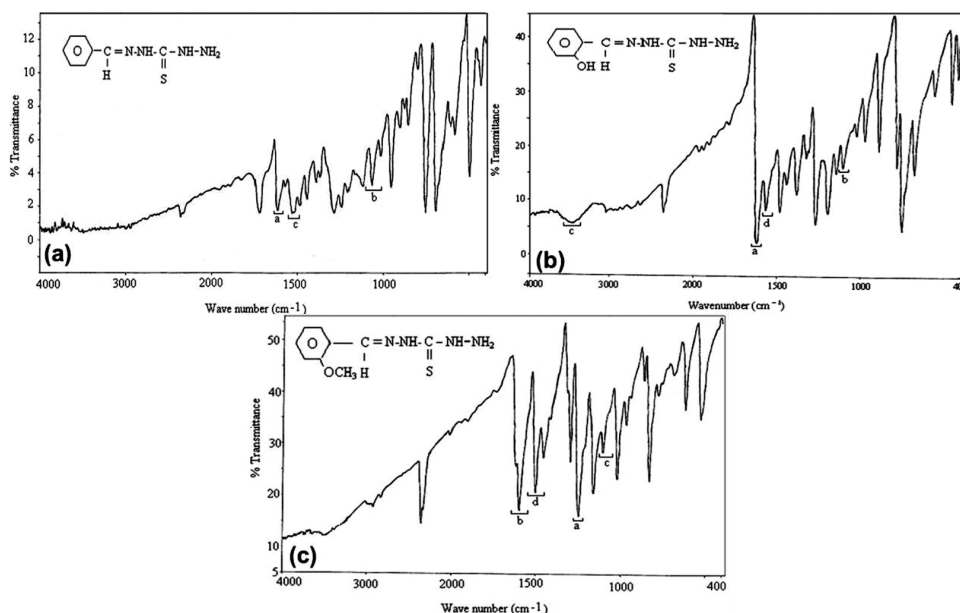
Fig. 1 (a) — FTIR spectrum of BTCH [[a]C=N stretch vibrations; [b]C=S stretch vibrations; [c]NH bending]; (b) FTIR spectrum of STCH [[a]C=N stretch vibrations; [b]C=S stretch vibrations; [c]C-OH stretching; [d]NH bending] and (c) FTIR spectrum of ATCH [[a]C-OC stretching; [b]C=N stretch vibrations; [c]C=S stretch vibrations; [d]NH bending.

Table 2 — Corrosion parameters obtained from weight loss measurements for the corrosion of carbon steel in 15% HCl in the absence and presence of different concentrations of inhibitors at 30°C for 6h immersion test

Inhibitor Conc. (ppm)	Weight loss (g)	Corrosion rate (mmpy)	Inhibition efficiency (%)	Surface coverage (θ)
Blank	1.6179	133.57	---	---
		BTCH		
500	0.4825	39.83	70.2	0.70
1000	0.3685	30.42	77.2	0.77
1500	0.2954	24.39	81.7	0.82
2000	0.2585	21.34	84.0	0.84
		STCH		
500	0.2798	23.10	82.7	0.83
1000	0.2042	16.86	87.4	0.87
1500	0.1355	11.19	91.6	0.92
2000	0.1305	10.77	91.6	0.92
		ATCH		
500	0.1763	14.55	89.1	0.89
1000	0.1236	10.20	92.4	0.92
1500	0.0719	5.94	95.6	0.96
2000	0.0665	5.49	95.6	0.96

Non-Electrochemical studies

Weight loss measurements

The percentage of inhibition efficiency and corrosion rate obtained from the weight loss method at different concentrations of inhibitors for the corrosion of carbon steel in 15% HCl for an immersion period of 6h at 30°C are given in Table 2. In the case of BTCH, inhibition efficiency increased with concentration from 500 to 2000 ppm. The maximum increase in inhibition efficiency (%) is found to be 84.0% for BTCH at 2000 ppm. This is due to increasing surface coverage by the inhibitor which leads to an increase in inhibition efficiency with increasing inhibitor concentration. Thus, an increase in inhibition efficiency with the concentration indicates that BTCH acts as an adsorption inhibitor. But in the case of ATCH and STCH, inhibition efficiency (IE) increased with the concentration of inhibitors. However, the maximum inhibition efficiency obtained at 1500 ppm is 91.6% and 95.6% for STCH and ATCH, respectively. Further increase in the concentration of inhibitor

beyond 1500 ppm does not cause any appreciable change in the performance of inhibitors. Hence, the optimum concentration required to achieve optimum inhibition was found to be 1500 ppm. Among the compounds investigated, IE is found to decrease in the following order:

ATCH > STCH > BTCH

In the case of ATCH, the presence of the methoxy group ($-OCH_3$) in the phenyl ring at the meta position certainly enhanced the electron density on the center of adsorption rather than in BTCH. But in the case of STCH, the ortho –OH group in the phenyl ring is likely to form an intermolecular hydrogen bonding with the polar N atom of the other molecule and thereby decreases the availability of some of the free lone pair electrons of the donor atom. This makes the performance of the molecule slightly poorer when compared to ATCH. The FTIR studies also confirm the presence of intermolecular hydrogen bonding of STCH (Fig. 1).

Electrochemical methods

Electrochemical polarization studies

The polarization behaviour of carbon steel in 15% HCl solution in the absence and presence of different concentrations (500 to 2000 ppm) of inhibitors at 30°C is shown in Fig. 2 (a-c). The extrapolation of Tafel straight lines allows the calculation of the corrosion current (I_{corr})[40]. The values of I_{corr}, the

corrosion potential (E_{corr}), Tafel slopes (b_c) and (b_a) and percentage inhibition efficiency are given in Table 3.

The addition of inhibitors in 15 % HCl solution does not show any significant change in E_{corr} suggesting that all the investigated compounds control the corrosion by controlling both anodic and cathodic reactions by blocking active anodic and cathodic sites on the metal surface. This indicates that the inhibition of corrosion of carbon steel in 15% HCl for all the compounds investigated was under mixed control. In BTCH, the maximum decrease in I_{corr} is observed at 2000 ppm. But, in the case of ATCH and STCH, the corrosion current (I_{corr}) is decreased with an increase in inhibitor concentration from 500 to 2000 ppm. Beyond the concentration of 1500 ppm, there is no appreciable effect on the decrease of corrosion current. This result is in good agreement with those obtained from weight loss measurements.

Electrochemical impedance measurements

Figure 3 (a-c) shows the impedance spectra for carbon steel in 15% HCl solution in the absence and presence of different concentrations of inhibitors at 30°C. The impedance spectra of BTCH and STCH (Fig. 3a&b), consists of a large capacitive loop at high frequencies (HFs) followed by a small inductive one at low frequency (LF) values. The high-frequency capacitive loop is usually related to the charge transfer of the corrosion process and the double layer
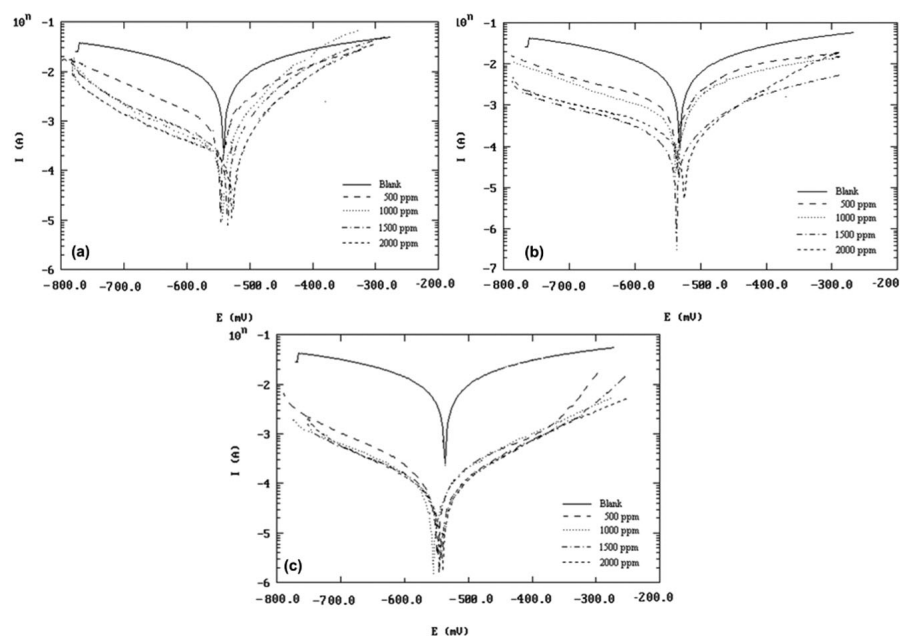

Fig. 2 — Electrochemical polarization curves for carbon steel in 15% HCl solution in the absence and presence of different concentrations of inhibitors (a) BTCH; (b) STCH and (c) ATCH.

Table 3 — Potentiodynamic polarization parameters for carbon steel in 15% HCl in the absence and presence of different concentrations of inhibitors at 30°C

| Inhibitor Conc. (ppm)	E_{corr} (mV vs SCE)	I_{corr} (mA/cm^2)	Tafel Slope (mV/decade)		Inhibition Efficiency (%)
			b_a	b_c	
Blank	−536	3.48	78	122	---
		BTCH			
500	-542	1.12	80	124	67.8
1000	-546	0.86	82	126	75.3
1500	-544	0.69	80	124	80.2
2000	-532	0.60	76	120	82.8
		STCH			
500	- 542	0.68	80	124	80.5
1000	- 538	0.53	78	122	84.8
1500	- 526	0.32	82	126	90.8
2000	- 522	0.31	80	124	91.0
		ATCH			
500	- 554	0.48	80	124	86.2
1000	- 558	0.32	82	126	90.8
1500	- 542	0.26	80	124	92.5
2000	- 534	0.25	84	128	92.8
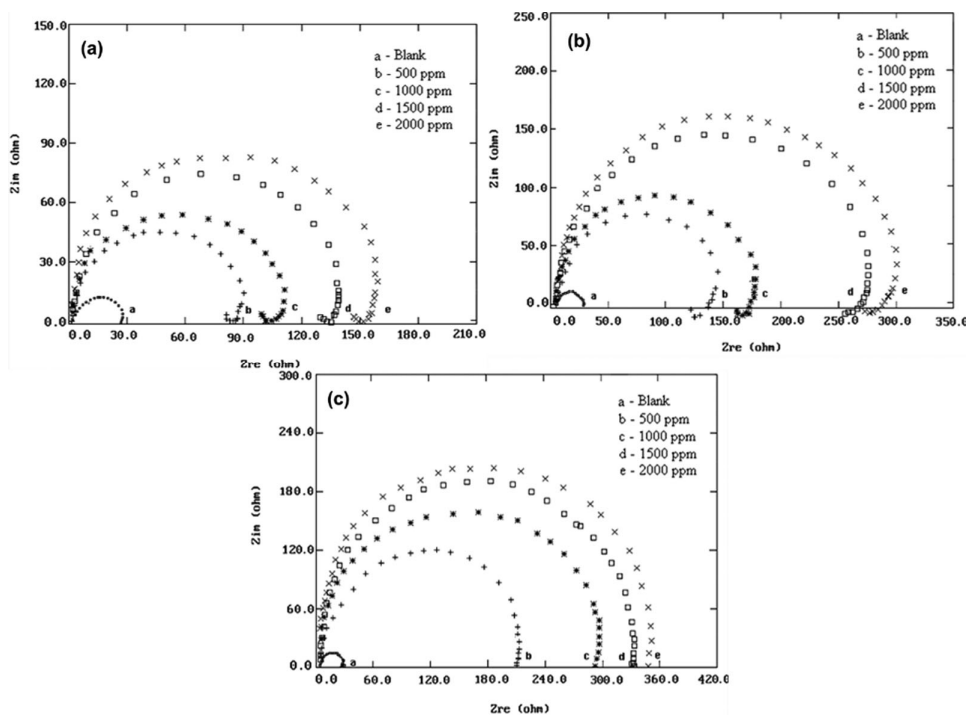
Fig. 3 — Impedance diagrams for carbon steel immersed in 15% HCl solution in the absence and presence of different concentrations of inhibitors (a) ATCH; (b) STCH and (c) BTCH.

behaviour, and the inductive loop may be attributed to the relaxation processes in the oxide film covering the electrode surface, which decreased the charge transfer resistance, R_t to lower values. But, in the case of ATCH, the well-defined semicircle (Fig. 3c) without much distortion shows that the corrosion of carbon steel is mainly controlled by a charge transfer process.

It is apparent from these plots that the impedance response of carbon steel in uninhibited HCl solution has significantly changed after the addition of inhibitors in the corrosive solution.

The characteristic parameters associated with the impedance diagram (R_t and C_{dl}) and % IE are given in Table 4. The inhibition efficiency increases with an

Table 4 — Impedance parameters for carbon steel in 15% HCl in the absence and presence of different concentrations of inhibitors at 30 °C

Inhibitor Conc (ppm)	R_t (Ω cm^2)	C_{dl} (μF/cm^2)	Inhibition Efficiency (%)
Blank	29	272	---
	BTCH		
500	87	89.62	66.7
1000	107	69.80	72.9
1500	136	58.00	78.7
2000	155	50.75	81.3
	STCH		
500	140	56.34	79.3
1000	169	46.65	82.8
1500	267	29.62	89.2
2000	278	28.21	89.6
	ATCH		
500	200	39.26	85.6
1000	296	26.58	90.2
1500	336	23.27	91.4
2000	348	22.61	91.7

Table 5 — Corrosion rate and inhibition efficiency for an optimum concentration of inhibitors on corrosion of carbon steel in 15% HCl at different temperatures for 1h obtained by weight loss method

Temperature (°C)	Blank	BTCH		STCH		ATCH	
	CR (mmpy)	CR (mmpy)	IE (%)	CR (mmpy)	IE (%)	CR (mmpy)	IE (%)
30	311.17	49.72	84.0	26.08	91.6	13.76	95.6
50	891.27	199.53	77.6	99.97	88.8	63.08	92.9
70	2511.87	707.95	71.8	354.86	85.9	281.75	88.8
90	6309.57	2311.89	63.4	1121.97	82.2	1023.38	83.8
110	14417.00	6153.18	57.3	3354.66	76.7	3009.83	79.1

increase in BTCH concentration and reached a maximum value at 2000 ppm. The C_{dl} decreases with the concentration of BTCH. This is due to the increased surface coverage by the inhibitor which leads to an increase in the inhibition efficiency. The decrease of this capacity with increasing inhibitor concentration may be attributed to a decrease in local dielectric constant and an increase in the thickness of the electrical double layer, suggesting that BTCH function by adsorption at the solution interface. An increase in STCH and ATCH concentrations up to 1500 ppm enhance the value of R_t and the values of double-layer capacitance are brought down to the maximum extent is due to the adsorption of inhibitor on the metal surface leading to the formation of the film in 15% HCl solution. A subsequent increase in the inhibitor concentration beyond 1500 ppm does not cause any significant decrease of C_{dl}, suggesting that for inhibitor concentration of 1500 ppm, the steel surface is totally covered by the inhibitor molecules. This result has also shown the same trend as those obtained from Tafel polarization and weight loss measurements.

Effect of temperature

The corrosion rate and inhibition efficiency with respect to temperature for compounds investigated are shown in Table 5. The logarithm of the corrosion rate is a linear function with 1/T. Using Arrhenius theory, activation energy can be calculated using equation (7)[41];

$$k = A \exp\left(\frac{-E_a}{RT}\right) \qquad \ldots (12)$$

where E_a is the apparent effective activation energy, R is the universal gas constant, T is the absolute temperature and A is the Arrhenius pre-exponential factor. Arrhenius plots for a log of corrosion rate vs 1/T gave straight lines (Fig. 4). Activation energies were calculated from the slopes of log corrosion rate vs 1/T curves. Gibbs adsorption energy, ΔG_A^o at different temperatures were calculated using equation (8)[42];

$$\Delta G_A^o = -RT \ln (55.5K) \qquad \ldots (13)$$

and K is given by following equation[43, 44];

$$K= \frac{\theta}{C\,(1-\theta)} \qquad\qquad \dots (14)$$

where θ is the degree of surface coverage on the metal surface obtained from weight loss measurements, C is the concentration of inhibitor in mol/L, T is the absolute temperature, R is the universal gas constant and K is the equilibrium constant.

The values of E_a and ΔG^{o}_{A} are shown in Table 6. The relationships between the temperature dependence of percentage inhibition efficiency of an inhibitor and the activation energy found in its presence can be classified into three groups according to temperature effects.

1. Inhibitors whose inhibition efficiency decreases with temperature increase, the value of the apparent activation energy, E_a is greater than that obtained in the uninhibited solution.
2. Inhibitors whose inhibition efficiency did not change with temperature variation, the apparent activation energy, E_a did not change in the presence or absence of inhibitors.
3. Inhibitors whose inhibition efficiency increases with temperature increase, the value of apparent
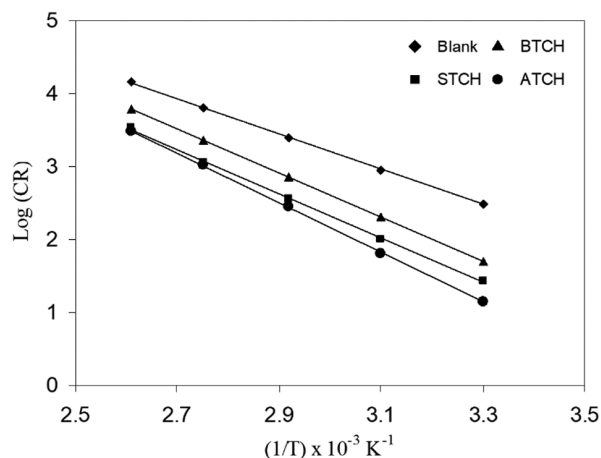

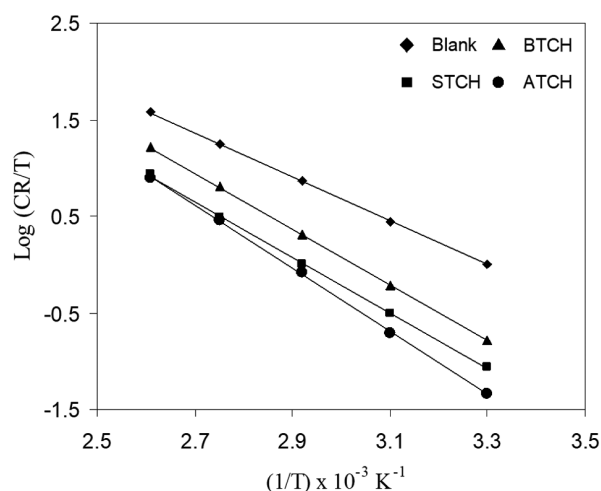Fig. 4 — Arrhenius plots for carbon steel immersed in 15% HCl solution in the absence and presence of an optimum concentration of inhibitors.

activation energy, E_a for the corrosion process is smaller than that obtained in the uninhibited solution.

From Table 5, the IE of inhibitors is found to decrease with an increase in temperature. The values of E_a for all the inhibitors are higher compared to pure acid and the decrease of IE with temperature is an indication of physical adsorption. The low and negative values of ΔG^{o}_{A} indicate the spontaneous adsorption of inhibitors on the surface of carbon steel. The negative values of ΔG^{o}_{A} also suggest the strong interaction of the inhibitor molecules onto the carbon steel surface. The ΔG^{o}_{A} value of all the inhibitors is less than -40 KJ/mol and the decrease in free energy of adsorption with temperature suggests physical adsorption of the inhibitors on the surface of carbon steel.

An alternative expression of the Arrhenius equation is the transition state is also given below[45];

$$\text{Rate} = \frac{RT}{Nh}\exp\left(\frac{\Delta S^{\circ}_{A}}{R}\right)\exp\left(\frac{-\Delta H^{\circ}_{A}}{RT}\right) \qquad \dots (15)$$

where, h is the Planck's constant, N is the Avogadro's number, ΔS^{o}_{A} is the entropy of activation and ΔH^{o}_{A} is the enthalpy of activation. A plot of log (CR / T) versus 1/T gave a straight line (Fig. 5), with a slope of $(-\Delta H^{o}_{A} / 2.303\ R)$ and an intercept of [log (R/Nh) + $(\Delta S^{o}_{A} /2.303R)$], from which the values of ΔS^{o}_{A} and ΔH^{o}_{A} was calculated and given in Table 6. Table 6 shows higher values obtained for E_a (65.20,58.23, 58.22) and ΔH^{o}_{A} (62.43, 55.25, 54.08) in the presence of inhibitors when compared to pure acid E_a (46.33) and ΔH^{o}_{A} (43.56), indicates higher inhibition efficiency. There is also a similarity between the increase in inhibition efficiency and the increase of E_a and ΔH^{o}_{A} values. The positive values of ΔH^{o}_{A} mean

Table 6 — Values of activation energy (E_a) and free energy of adsorption - ΔG^{o}_{A} and thermodynamic activation parameters for carbon steel in 15% HCl in the absence and presence of an optimum concentration of inhibitors at different temperatures

Inhibitor	E_a (kJ mol^{-1})	$-\Delta G^{o}_{A}$ (kJ mol^{-1})					ΔH^{o}_{A} (kJ mol^{-1})	ΔS^{o}_{A} (J mol^{-1}K^{-1})	Q_A (kJ mol^{-1})
		30°C	50°C	70°C	90°C	110°C			
Blank	46.33	---	---	---	---	---	43.56	-53.86	---
BTCH	58.22	26.75	27.40	28.22	28.70	29.47	54.08	-28.94	-14.46
STCH	58.23	28.39	29.41	30.34	31.42	32.08	55.25	-35.85	-16.45
ATCH	65.20	30.49	31.14	31.64	32.20	32.98	62.43	-44.59	-21.09

that the dissolution reaction is an exothermic process and the dissolution of steel is difficult. The values of entropy of adsorption, ΔS_A^o in the presence of the inhibitors are large and negative. This indicates that the activated complex in the rate-determining step represents an association rather than a dissociation step, meaning that a decrease in disordering takes place on going from reactants to the activated complex.

The heat of adsorption (Q_A) of the inhibitor can be calculated using equation (10);

Fig. 5 — Plot of log (CR/T) vs 1/T for carbon steel immersed in 15% HCl solution in the absence and presence of an optimum concentration of inhibitors.

$$Q_A = 2.303R\left[\log\left(\frac{\theta_2}{1-\theta_2}\right) - \log\left(\frac{\theta_1}{1-\theta_1}\right)\right] \times \frac{T_1 T_2}{T_2 - T_1} \text{ kJmol}^{-1} \quad \ldots (16)$$

where θ_1 and θ_2 are the degrees of surface coverage at temperatures T_1 and T_2 (K) respectively. Negative Q_A values indicate physical adsorption on the metal surface.

Synergistic effect of acidizing inhibitors with KI /CuI on corrosion inhibition

The values of inhibition efficiency and synergism parameters obtained from weight loss measurements in 15% HCl at 110°C containing an optimum concentration of inhibitors combined with different concentrations of KI and CuI are given in Tables 7 and 8. Experimental results suggested that the addition of different concentrations of KI and CuI to the inhibited solution increases the IE and the degree of surface coverage (θ) at all concentrations. The optimum concentration required to achieve the maximum inhibition was found to be 1500 ppm of inhibitor with 0.3% KI and 1500 ppm of inhibitor with 0.02% CuI for all other inhibitors except BTCH. For BTCH the optimum concentration required to achieve the maximum inhibition was found to be 2000 ppm of inhibitor with 0.3% KI and 2000 ppm of inhibitor with 0.02% of CuI. The inhibition efficiency of inhibitors was found to be more effective in the presence of CuI than in the presence of KI. This behaviour was attributed to the results of the synergistic effect between iodide ions and inhibitors.

Table 7 — Inhibition efficiency and synergism parameter (S_θ) obtained from weight loss measurements for an optimum concentration of inhibitors combined with different concentrations of KI in 15% HCl at 110°C for 1h immersion test.

Name of the inhibitor	Inhibitor conc. (ppm)	KI Conc. (%)	Inhibition Efficiency (%)	Synergism parameter (S_θ)
BTCH	2000	0.0	57.3	---
		0.1	63.4	0.92
		0.2	72.6	1.18
		0.3	79.7	1.54
		0.4	77.1	1.44
		0.5	74.2	1.34
STCH	1500	0.0	76.7	---
		0.1	80.6	0.95
		0.2	83.9	1.10
		0.3	87.2	1.33
		0.4	85.8	1.26
		0.5	82.6	1.08
ATCH	1500	0.0	79.1	---
		0.1	83.8	1.02
		0.2	86.4	1.09
		0.3	90.5	1.45
		0.4	87.0	1.24
		0.5	85.1	1.14

Table 8 — Inhibition efficiency and synergism parameter (S_θ) obtained from weight loss measurements for an optimum concentration of inhibitors combined with different concentrations of CuI in 15% HCl at 110°C for 1h immersion test.

Name of the inhibitor	Inhibitor conc. (ppm)	KI Conc. (%)	Inhibition efficiency (%)	Synergism parameter (S_θ)
BTCH	2000	0.00	57.3	---
		0.01	76.2	0.93
		0.02	90.0	1.88
		0.03	86.1	1.78
		0.04	83.4	1.62
STCH	1500	0.00	76.7	---
		0.01	87.6	0.98
		0.02	93.0	1.46
		0.03	86.1	0.97
		0.04	82.6	0.84
ATCH	1500	0.00	79.1	---
		0.01	88.7	0.82
		0.02	94.4	1.64
		0.03	93.1	1.53
		0.04	91.6	1.27

The synergism parameter (S_θ) was calculated from the data of weight loss measurements using the relationship given by Aramaki and Hackermann using equation (11)[46];

$$S_\theta = \frac{1 - \theta_{1+2}}{1 - \theta'_{1+2}} \qquad \ldots (17)$$

Where $\theta_{1+2} = \theta_1 + \theta_2 - \theta_1\theta_2$, θ_1 is the surface coverage by anion, θ_2 is the surface coverage by cation and θ'_{1+2} is the measured surface coverage by both anion and cation.

The values of S_θ increases with the concentration of KI and CuI and a maximum S_θ value is obtained at 0.3% of KI and 0.02% of CuI, which are more than unity. The enhanced IE caused by the addition of iodide ions with the inhibitors is due to only the synergistic effect.

Hydrogen permeation studies

Permeation current vs time curves for carbon steel in 15% HCl in the absence and presence of inhibitors are shown in Fig. 6 and their corresponding values are given in Table 9. It can be that a definite correlation exists between the extent of corrosion inhibition and the percentage decrease in permeation current.

Adsorption isotherm

The values of surface coverage (θ) corresponding to different concentrations of inhibitors obtained from weight loss measurements at 30°C have been used to explain the best isotherm to determine the adsorption process. Using the values of coverage (θ), Langmuir,
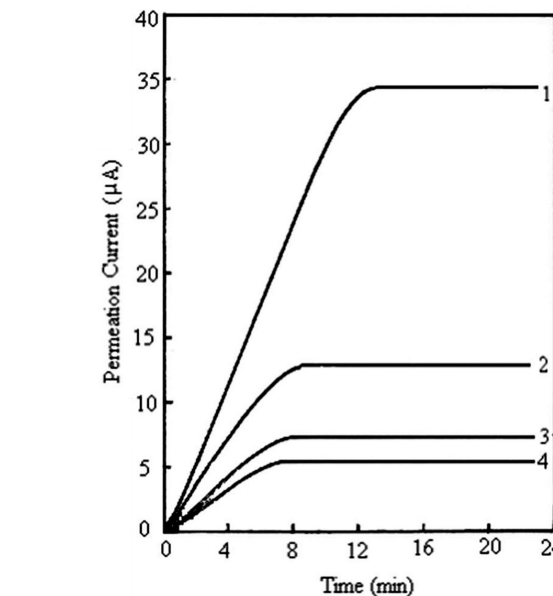

Fig. 6 — Hydrogen permeation current vs time plots for carbon steel in 15% HCl solution in the absence and presence of an optimum concentration of inhibitors (1) Blank, (2) BTCH (1500 ppm), (3) STCH (2000 ppm), (4) ATCH (1500 ppm).

Frumkin or Temkin isotherms were attempted for all the compounds under study. Langmuir isotherm was tested by plotting C/θ vs C. A straight-line relationship (Fig. 7) was obtained in all the cases suggesting that all these compounds obey Langmuir adsorption isotherm where θ and C (inhibitor's concentration in the bulk of the solution) are related to each other via the equation (12).

$$\theta = \frac{KC}{(1 + KC)} \qquad \ldots (12)$$

Table 9 — Values of hydrogen permeation current for the corrosion of carbon steel in 15% HCl alone and in the presence of inhibitors

Name of the Inhibitor	Inhibitor Conc. (ppm)	Permeation current (μA)	Decrease in permeation current (%)
Blank	---	34.5	---
BTCH	2000	13.2	61.7
STCH	1500	7.4	78.5
ATCH	1500	5.4	84.4
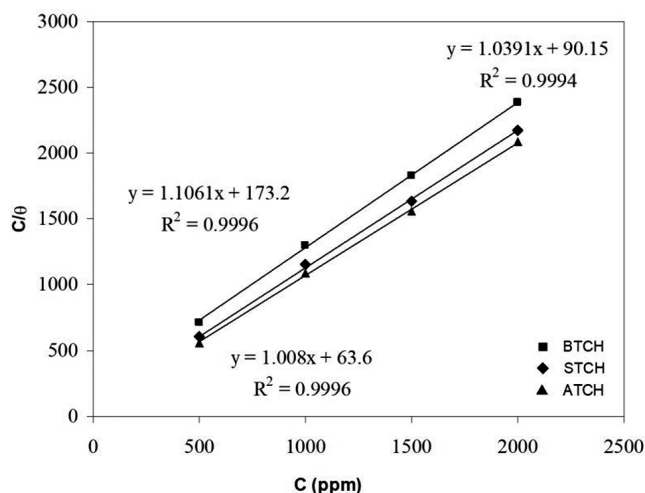
Fig. 7 — Temkin adsorption isotherm plots for the adsorption of different concentrations inhibitors on the surface of carbon steel in 15% HCl solution.

Rearrangement gives the equation (13)

$$\frac{C}{\theta} = \left(\frac{1}{K}\right) + C \qquad \ldots (13)$$

where K is the equilibrium constant of the adsorption process. For all the inhibitors slope of the straight line is equal to unity. So, it could be concluded that inhibitors are adsorbed at the steel surface following Langmuir isotherm without interaction between the adsorbed molecules. Fig. 7 shows the isotherm plots of the inhibitors studied for their adsorption on carbon steel in 15% HCl solution.

Surface Examination Studies

FTIR Spectral Studies

The FTIR spectrum obtained for the carbon steel immersed in 15% HCl solution is shown in Fig. 8(a). The spectrum of the film formed on the surface of the carbon steel immersed in 15% HCl solution containing an optimum concentration of inhibitors are given in Fig. 8(b-d). It is clear from Fig. 8(b-d) that the peaks corresponding to >C=S- stretching frequency of organic compounds. This suggests that the sulphur atom is coordinated to Fe^{2+} resulting in the formation of a Fe^{2+} - inhibitor complex on the metal surface. It is also inferred from the spectrum that C = S stretching frequency decreased from 1068 cm^{-1} to 1051 cm^{-1}, 1110 cm^{-1} to 1050 cm^{-1} and 1108 cm^{-1} to 1052 cm^{-1} for BTCH, STCH and ATCH respectively confirming
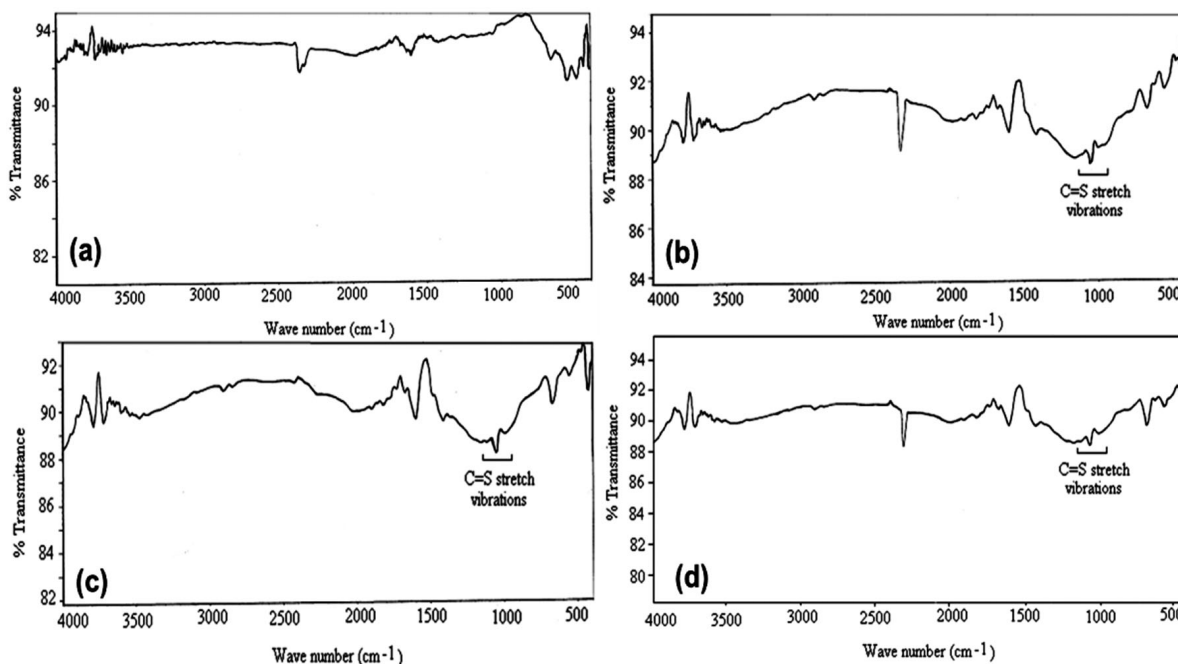

Fig. 8 — FT-IR Spectrum of the surface of carbon steel immersed in 15% HCl alone and in a solution containing an optimum concentration of inhibitors (a) Blank; (b) BTCH; (c) STCH and (d) ATCH.

the bond formation through $>C = S$ group between the inhibitors and the carbon steel surface.

UV-Visible Reflectance Studies

The inhibition of corrosion of carbon steel in 15% HCl solution in the presence of inhibitors may be due to the formation of film on the metal surface, is also supported by UV-Visible reflectance studies, carried out by using a spectrophotometer for carbon steel specimen immersed in 15% HCl alone and for specimens immersed in 15% HCl solution containing the optimum concentration of inhibitors. A comparison of reflectance curves drawn on a uniform scale for polished carbon steel specimen, carbon steel specimen immersed in 15% HCl alone and in the presence of inhibitors is shown in Fig. 9. The percentage of reflectance is maximum for a polished specimen and it has been reduced considerably in the case of a specimen immersed in 15% HCl alone. However, in the case of specimens immersed in 15% HCl solution containing an optimum concentration of inhibitors, reflectance has been reduced to only a very small extent. This shows that surface characteristics are not altered very much, due to the formation of a film on the metal surface.

SEM studies

Surface examination studies through scanning electron microscopy at a magnification of X1000 for the metal specimens dipped in 15% HCl at 30°C for 6h in the absence and presence of the optimum concentration of inhibitors are shown in Fig. 10 (a–d). In the absence of inhibitors, the corroded metal surface with etched grain boundaries and corrosion products are clearly seen (Fig. 10a). In the presence of inhibitors such as STCH and ATCH (Fig. 10c & d), the fully protected metal surface without any corrosion products is observed. Only the original
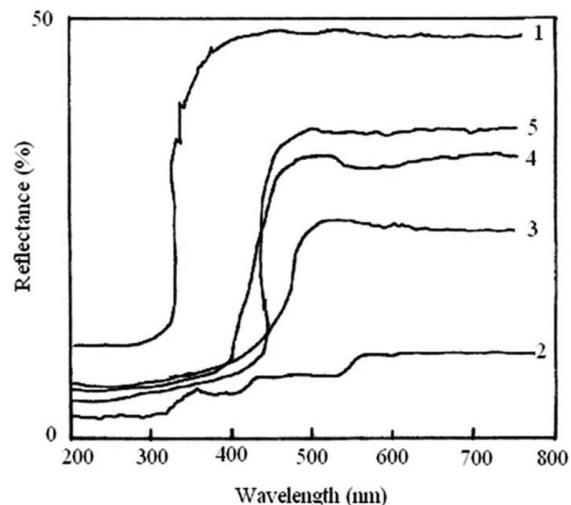

Fig. 9 — UV-Visible reflectance curves for carbon steel specimens in 15% HCl solution in the absence and presence of an optimum concentration of inhibitors (1) Polished, (2) Blank, (3) BTCH (1500 ppm), (4) STCH (1500 ppm), (5) ATCH (2000 ppm).
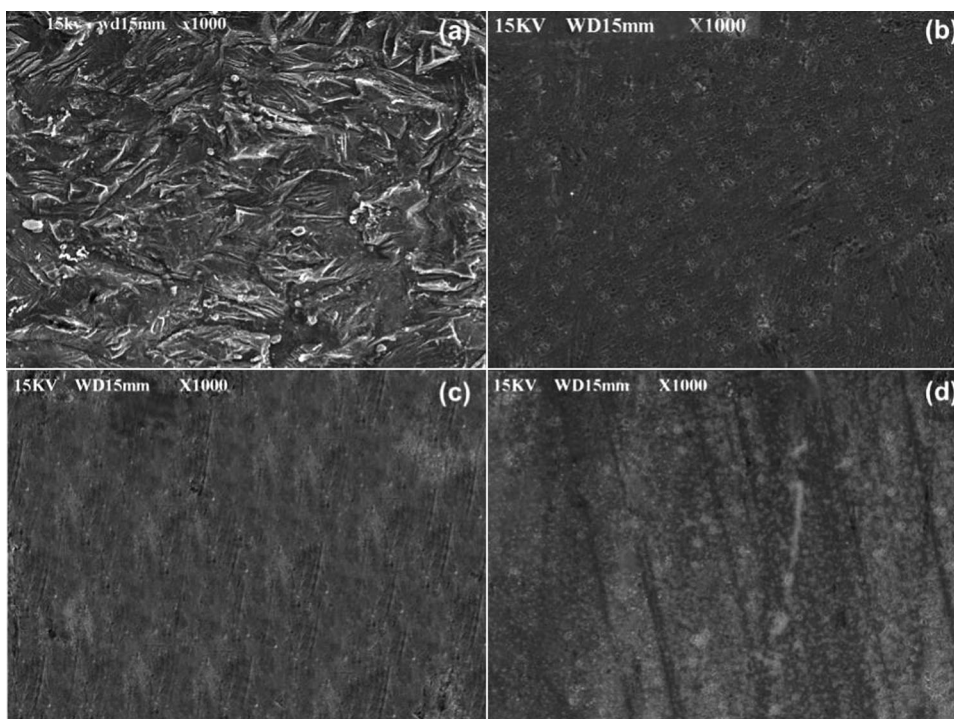

Fig. 10 — SEM Photograph of carbon steel immersed 15% HCl alone and the solution containing an optimum concentration of inhibitors (a) Blank (b) BTCH (c) STCH and (d) ATCH.

surface defects of the metal specimens such as scratches, notches, and some dents are seen. In the presence of BTCH traces of corrosion products are visible with some white patches on the metal surface due to very restricted corrosion (Fig. 10b).

Theoretical studies

The quantum chemical calculations are performed to further understand and validate the corrosion inhibition mechanism of BTCH, STCH, and ATCH. The optimized geometric structures and distribution of HOMO and LUMO of the respective inhibitors are shown in Fig. 11. It can be observed that the prepared thiocarbohydrazides have different HOMO and LUMO distributions (Fig. 11). The aromatic ring of BTCH does not contribute to the HOMO distribution which may be due to the absence of a heteroatom-containing functional group. The higher value of E_{HOMO} of an inhibitor denotes its strong electron-donating ability for the empty molecular orbitals of the metal and thereby facilitates the adsorption (chemisorption) on the metal surface. The E_{LUMO} is related to the electron-accepting ability of the inhibitor molecules and lower E_{LUMO} values denote their greater tendency to acceptance of electrons from the metal surface.

The lower energy gap (ΔE) between the E_{HOMO} and E_{LUMO} favours high corrosion inhibition. Table 10 denotes the calculated quantum chemical parameters of the prepared acidizing inhibitors. The values of E_{HOMO} and ΔE follow the order of ATCH > STCH > BTCH and ATCH < STCH < BTCH, respectively. It indicates that the inhibition efficiency is in the following order; ATCH > STCH > BTCH, which has good agreement with the experimental results. Other parameters such as global electronegativity (χ), global hardness (η) and global softness (σ) are the indicator of the reactivity and stability of the inhibitors. The energy gap (ΔE) is lower for the softer molecules and higher for harder molecules. The ATCH with higher σ and lower η exhibited higher corrosion inhibition efficiency. The electronegativity (χ) is a reactivity index which is inversely related to the electron donation of the molecule. The values of χ and ΔN are in the order of ATCH<STCH<BTCH and ATCH>STCH>BTCH, respectively, which are consistent with the experimental results. This can be further supported by the effect of electron-donating ability of the groups -OCH$_3$ and -OH

(a) 1-benzylidine-3-thiocarbohydrazide (BTCH)

(b) 1-salicylidine-3-thiocarbohydrazide (STCH)

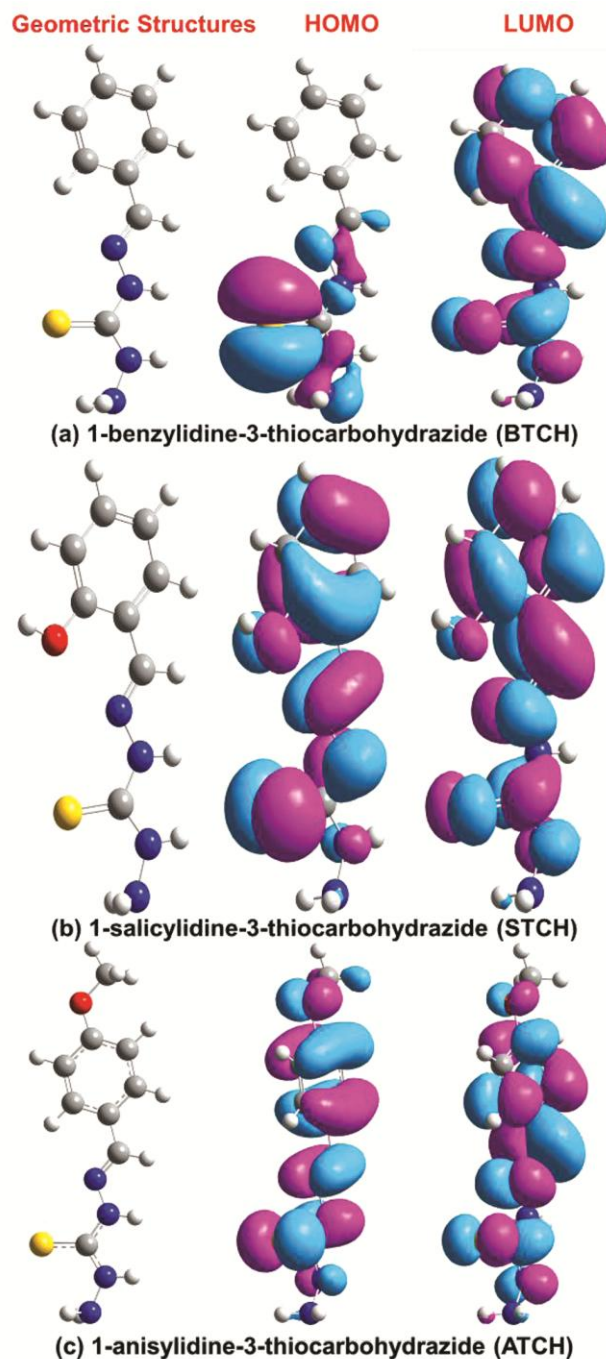(c) 1-anisylidine-3-thiocarbohydrazide (ATCH)

Fig. 11 — Optimized geometric structures, HOMO and LUMO density distribution of (a) 1-benzylidene-3-thiocarbohydrazide; (b) 1-salicylidene-3-thiocarbohydrazide and (c) 1-anisylidene-3-thiocarbohydrazide.

attached to the aromatic ring of the ATCH and STCH, respectively. The order of electron-donating abilities of the functional group, -OCH$_3$ > -OH is consistent with the experimental corrosion performance of their corresponding molecules[47, 48].

Table 10 — Calculated quantum chemical parameters for the prepared corrosion inhibitors using DFT-B3LYP/6-31G

Parameters	Compounds		
	BTCH	STCH	ATCH
E_{HOMO} (eV)	-5.9895	-5.86786	-5.70922
E_{LUMO} (eV)	-1.61744	-1.49880	-1.44275
ΔE (eV)	4.37205	4.36906	4.26647
χ (eV)	3.80347	3.68333	3.57598
η	2.186027	2.18453	2.133236
σ	0.45745	0.45776	0.46877
ΔN	0.731127	0.75912	0.80254

STCH, respectively. The order of electron-donating abilities of the functional group, $-OCH_3 > -OH$ is consistent with the experimental corrosion performance of their corresponding molecules[47, 48].
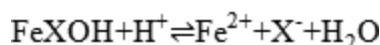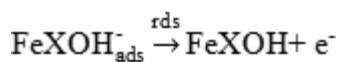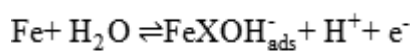
Discussion

Weight loss and electrochemical measurements have been employed to study the behaviour of carbon steel in 15% HCl solution, in the absence and presence of organic inhibitors. The results indicate that the values of inhibition efficiency increased markedly with the increase of inhibitor concentration, indicating that a higher coverage of inhibitor on the metal surface was obtained in a solution with 1500 ppm of STCH and ATCH and 2000 ppm of BTCH respectively. The very high inhibition efficiency of compounds is understandable from the molecular structure. Effective adsorption on the metal surface is due to the presence of N and S atoms, -C=N group, $-OCH_3$ group, -OH group and aromatic rings.

Many mechanisms have been proposed for the inhibition of metal corrosion by organic inhibitors. Generally, it has been assumed that the first stage in the action mechanism of the inhibitor in the aggressive acid media is based on its adsorption on the metal surface. The processes of adsorption of inhibitors are influenced by the nature of the organic inhibitor, the distribution of charge in the molecule, the type of aggressive electrolyte and the type of interaction between organic molecules and the metallic surface.

Halide ions are good ligands as they exhibit a low electronegativity (less than 3.5). Electronegativity decreases from Cl^- to I^- ($Cl^- = 3.16$, $Br^- = 2.96$, $I^- = 2.66$), while the covalent radius increases from Cl^- to I^- ($Cl^- = 0.99$Å$^°$, $Br^- = 1.14$ Å$^°$, $I^- = 1.33$Å$^°$). Halide ions enhance the performance of amine base organic corrosion inhibitors in acid solution. The inhibition

efficiency of halides increases in the order: $Cl^- < Br^- < I^-$, which seems to indicate that the radii of halogen ions may also play a role. With an increasing ionic radius of halides, electron cloud on the atom is facilitated, i.e. they are deformed more easily when adsorbed on a metal surface. Therefore I^- (radius = 1.33 A$^°$) is favourable for adsorption than the Br^- (radius = 1.14 A$^°$) and Cl^- (radius = 0.99 A$^°$). Halide ions inhibit anodic dissolution of iron by replacing some adsorbed catalytic OH^- ions on the metal surface. Iron dissolution in acidic chloride solution may thus be generalized for all the halides as follows;

$$Fe + H_2O \rightleftharpoons FeXOH^-_{ads} + H^+ + e^-$$

$$FeXOH^-_{ads} \xrightarrow{rds} FeXOH + e^-$$

$$FeXOH + H^+ \rightleftharpoons Fe^{2+} + X^- + H_2O$$

where X represents the halide ion.

Corrosion inhibition synergism results from the increased surface coverage arising from ion-pair interactions between the organic inhibitor and the halide ions. Two possible mechanisms account for the metal surface. According to the first mechanism, the ion-pairs are formed in the bulk of the solution and then adsorbed from the solution on to the metal surface as follows;

$$Y_s + X_s \rightarrow (YX)_s$$
$$(YX)_s \rightarrow (YX)_{ads}$$
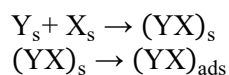
In the second mechanism, the halide ion is first adsorbed on the metal surface and the inhibitor is then drawn into the double layer by the adsorbed halide ion such that the ion-pair formation occurs directly on the metal surface.

$$X_s \rightarrow X_{ads}$$
$$Y_s + X_{ads} \rightarrow (YX)_{ads}$$
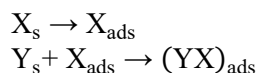
where Y_S, X_S and $(YX)_S$ represent the inhibitor, halide ion and ion-pair, respectively in bulk solution and Y_{ads}, X_{ads} and $(YX)_{ads}$ refer to the same species in the adsorbed state.

The synergistic inhibition effect in the present work can be explained as follows; The strong chemisorption of iodide ions on the metal surface is responsible for the synergistic effect of iodide ions in combination with the protonated cations of the inhibitors. The cations of the inhibitors are then adsorbed by coulombic attraction on

hydrochloric acid solutions. Extended acid–metal contact times are also possible when using the organo-metal halide inhibitor system. The metal cation, as well as the halide anion, may be involved in the improved corrosion inhibition when copper iodide is used in conjunction with an amine base organic corrosion inhibitor.

Conclusion

All the chosen three inhibitors such as BTCH, STCH and ATCH inhibit the corrosion of carbon steel in 15% HCl solution and control both anodic and cathodic reactions by blocking the active sites of the steel surface and are thus inhibitors of mixed type. The adsorption of inhibitors on carbon steel obeys Langmuir adsorption isotherm. The values of S_θ which are more than unity suggest that the enhanced IE caused by the addition of iodide ions to the inhibitors is due to the synergistic effect. The theoretical results are consistent with the experimental corrosion performance of the corresponding molecules. Hence, among the studied three inhibitors, STCH and ATCH can be effectively used as acidizing inhibitors for oil-well applications.

Conflict of interest

The authors declare no competing financial interest.

References

1   Furtado L B, Nascimento R C, Seidl P R, Guimarães M J O C, Costa L M, Rocha J C & Ponciano J A C, *J Mol Liq*, 284 (2019) 393.
2   Fouda A S, Mostafa H A, El-Taib F & Elewady G Y, *Corros Sci*, 47 (2005) 1988.
3   Rajendran S, Srinivasan R, Dorothy R, Umasankareswari T & Al-Hashem A, *Int J Corros Scale Inhib*, 8 (2019) 437.
4   Prabha S S, Rathish J, Dorothy R, Brindha G, Pandiarajan M, Al-Hashem A & Rajendran S, *Eur Chem Bull*, 3 (2014) 300.
5   Ituen E, Mkpenie V & Dan E, *Surf Interfaces*, 16 (2019) 29.
6   Du J, *Anti Corros Methods Mater*, 66 (2019) 1.
7   Zhang H Y, Lei Y Y, Li J Y, Zhang Y Z, Di Z G, Wu P P, Li P, Qu H M & Wang M L, *Corros*, 75 (2019) 809.
8   Obaid A Y, Ganash A A, Qusti A H, Elroby S A & Hermas A A, *Arabian J Chem*, 10 (2017) S1276.
9   Cui X, Zhu G, Pan Y, Shao Q, Zhao C, Dong M, Zhang Y & Guo Z, *Polym*, 138 (2018) 203.
10 Gojić M, *Corros Sci*, 43 (2001) 919.
11 Wang L, Yin G J & Yin J G, *Corros Sci*, 43 (2001) 1197.
12 Ashassi-Sorkhabi H, Shaabani B & Seifzadeh D, *Electrochim Acta*, 50 (2005) 3446.
13 Abdel-Rehim S S, Khaled K F & Abd-Elshafi N S, *Electrochim Acta*, 51 (2006) 3269.
14 Zhang Y, Zhao M, Zhang J, Shao Q, Li J, Li H, Lin B, Yu M, Chen S & Guo Z, *J Polym Res*, 25 (2018) 130.
15 Sathiya Priya A R, Muralidharan V S & Subramania A, *Corros*, 64 (2008) 541.
16 Hollis G, Davies D R, Johnson T M & *Wade L G, Organic chemistry*, 6th edition, L.G. Wade Jr. : test item file, Pearson Prentice Hall, Upper Saddle River, N.J., (2006).
17 Singh A, Ansari R K, Quraishi A M & Lgaz H, *Mater*, 12 (2018).
18 Kang H, Cheng Z, Lai H, Ma H, Liu Y, Mai X, Wang Y, Shao Q, Xiang L, Guo X & Guo Z, *Sep Purif Technol*, 201 (2018) 193.
19 Umoren S A, Solomon M M, Ali S A & Dafalla H D M, *Mater Sci Eng C*, 100 (2019) 897.
20 20 Ituen E B, Solomon M M, Umoren S A & Akaranta O, *J Pet Sci Eng*, 174 (2019) 984.
21 Yang Z, Wang Y, Zhan F, Wang R, Chen W, Ding M & Hou B, NACE - Int Corros Conf Ser, (2019).
22 Singh P, Quraishi M A, Gupta S L & Dandia A, *J Taibah Univ Sci*, 10 (2016) 139.
23 Tawfik S M, *J Mol Liq*, 207 (2015) 185.
24 Prabhu R A, Venkatesha T V, Shanbhag A V, Kulkarni G M & Kalkhambkar R G, *Corros Sci*, 50 (2008) 3356.
25 Bashir S, Sharma V, Singh G, Lgaz H, Salghi R, Singh A & Kumar A, *Metall Mater Trans A*, 50 (2018) Please tell me pages number.
26 Chopra R, Kansal K, Kumar R & Singh G, *J Failure Anal Prev*, 18 (2018) 1411.
27 Kumar R, Singh G, Kim H & Reddicherla U, *J Mol Liq*, 268 (2018) Please tell me pages number.
28 Boucherit L, Al-Noaimi M, Daoud D, Douadi T, Chafai N & Chafaa S, *J Mol Struct*, 1177 (2019) 371.
29 Hamadi L, Mansouri S, Oulmi K & Kareche A, *Egypt J Pet*, 27 (2018) 1157.
30 Ji G, Shukla S K, Dwivedi P, Sundaram S & Prakash R, *Ind Eng Chem Res*, 50 (2011) 11954.
31 Zhang Q B & Hua Y X, *Electrochim Acta*, 54 (2009) 1881.
32 Li Q, Liu H, Zhang S, Zhang D, Liu X, He Y, Mi L, Zhang J, Liu C, Shen C & Guo Z, *ACS Appl Mater Interfaces*, 11 (2019) 21904.
33 Yoo S H, Kim Y W, Chung K, Kim N K & Kim J S, *Ind Eng Chem Res*, 52 (2013) 10880.
34 Yadav M, Behera D, Kumar S & Sinha R R, *Ind Eng Chem Res*, 52 (2013) 6318.
35 Subramania A, Kalyana Sundaram N T, Sathiya Priya R, Saminathan K, Muralidharan V S & Vasudevan T, *J Appl Electrochem*, 34 (2004) 693.
36 Subramania A, Kalyanasundaram N, Sathiyapriya R, Muralidharan V & Vasudevan T, *Bull Electrochem*, 20 (2004)49.
37 Singh P, Ebenso E E, Olasunkanmi L O, Obot I B & Quraishi M A, *J Phy Chem C*, 120 (2016) 3408.
38 Zheng X, Zhang S, Gong M & Li W, *Ind Eng Chem Res*, 53 (2014) 16349.

39 Kumar S, Sharma D, Yadav P & Yadav M, *Ind Eng Chem Res*, 52 (2013) 14019.

40 Zhu G, Cui X, Zhang Y, Chen S, Dong M, Liu H, Shao Q, Ding T, Wu S & Guo Z, *Polym*, 172 (2019) 415.

41 Yadav D K & Quraishi M A, *Ind Eng Chem Res*, 51 (2012) 14966.

42 Mishra A, Verma C, Lgaz H, Srivastava V, Quraishi M A & Ebenso E E, *J Mol Liq*, 251 (2018) 317.

43 Agrawal R & Namboodhiri T K G, *Corros Sci*, 30 (1990) 37.

44 Tang L, Mu G & Liu G, *Corros Sci*, 45 (2003) 2251.

45 Abd El Rehim S S, Hassan H H & Amin M A, *Mater Chem Phys*, 70 (2001) 64.

46 Yousefi A, Javadian S & Neshati J, *Ind Eng Chem Res*, 53 (2014) 5475.

47 Singh P, Kumar M, Quraishi M A, Haque J & Singh G, *ACS Omega*, 3 (2018) 11151.

48 Hari Kumar S & Karthikeyan S, *Ind Eng Chem Res*, 52 (2013) 7457.